Journal of Hazardous Materials 166 (2009) 523–530

Contents lists available at ScienceDirect

Journal of Hazardous Materials

journal homepage: www.elsevier.com/locate/jhazmat

Simultaneous removals of NO_x, HC and PM from diesel exhaust emissions by dielectric barrier discharges

Chong-Lin Song*, Feng Bin, Ze-Min Tao, Fang-Cheng Li, Qi-Fei Huang

State Key Laboratory of Engines, Tianjin University, Tianjin 300072, China

ARTICLE INFO

Article history:
Received 27 June 2008
Received in revised form
19 November 2008
Accepted 19 November 2008
Available online 28 November 2008

Keywords:
Dielectric barrier discharge
Diesel engine
Particulate matter
Hydrocarbon
Nitrogen oxide

ABSTRACT

The main target of this work is to characterize the abatements of particulate matter (PM), hydrocarbons (HC) and nitrogen oxides (NO_x) from an actual diesel exhaust using dielectric barrier discharge technology (DBD). The effects of several parameters, such as peak voltage, frequency and engine load, on the contaminant removals have been investigated intensively. The present study shows that for a given frequency, the removals of PM and HC are enhanced with the increase of peak voltage and level off at higher voltage, while in the range of higher voltages a decline of NO_x removal efficiency is observed. For a given voltage, the maximums of specific energy density (SED) and removal efficiency are attained at resonance point. The increase of peak voltage will result in a significant decrease of energy utilization efficiency of DBD at most engine loads. Alkanes in soluble organic fraction (SOF) are more readily subjected to removals than polycyclic aromatic hydrocarbons (PAHs).

1. Introduction

Due to the lower operating costs, higher thermal efficiency as well as longer durability compared with gasoline engines, diesel engines have been widely employed as the major propulsion source for heavy-duty transportations and off-road applications. Besides hydrocarbons (HC) and carbon monoxide (CO) emissions, they however emit 2–20 times more nitrogen oxides (NO_x) and roughly 30–100-fold higher particulate matter (PM) than gasoline engines [1]. Hence the global concern over the exhaust pollutants of diesel engine has triggered awareness focused on the development of diesel exhaust after treatment technology. Presently, selective catalytic reduction (SCR) and diesel particulate filters (DPF) have been accepted on diesel engine in compliance with the latest regulated standards. Unfortunately, the common problem with SCR appears to be their narrow temperature operation bands, the small residence time of the exhaust gas, catalyst poisoning, ammonia leakage and the discharge of catalyst mass under the high temperature conditions [2–4]. As for DPF, the major challenges are the low collection efficiency for nanosized particles, their regeneration and the complexity in operation, which lead to high-fuel consumption, the possibility of exhaust backpressure as well as high maintenance costs [5,6].

Combined with the unique advantages of rapid reaction, high electron energies and easy operations, non-thermal plasma (NTP) processing has currently been investigated intensively as a promising technology of diesel engine after treatment to abate PM, HC and NO_x. NTP technologies mainly include surface discharge [7], electron beam irradiation [8], pulsed corona discharge (PCD) [9] and dielectric barrier discharge (DBD) [10]. Numerous experiments have been carried out to reduce PM, HC and NO_x from diesel exhaust emissions using these approaches.

Yao et al. [11] reported that an uneven discharge reactor, combining DBD with PCD during discharges, could achieve PM removal efficiency of 67% at 300 W, and the energy efficiency was typically in a range of 3–10.6 g/kWh corresponding to the energy density of 2–16 J/L. Willems et al. [12] evaluated the PM reduction in a packed-bed plasma system with the experimental results indicating that 90% removal efficiency based on smoke measurements was determined at an energy density of 25 J/L for relatively small velocities. Besides, Sato et al. [5] developed a PM electrostatic precipitator, integrating a dust pocket with a DBD device installed in the downstream. Conductive particles touching to the mesh of the dust pocket are pulled into the high electric field region, and oxidized by the barrier discharges. After operating the experiment for a long period, the collection efficiency could be kept at almost the same level of 99% up to 180 min.

With respect to NO_x abatement, Koizumi et al. [13] and Herling et al. [14] demonstrated that NTP processing alone has an oxidative potential to convert NO to NO_2 effectively. However, the task of NO_2 reduction would be faced with the difficulty that NTP process-

* Corresponding author. Tel.: +86 22 27406840x8020; fax: +86 22 27403750.
E-mail address: songchonglin@tju.edu.cn (C.-L. Song).

0304-3894/$ – see front matter © 2008 Elsevier B.V. All rights reserved.
doi:10.1016/j.jhazmat.2008.11.068

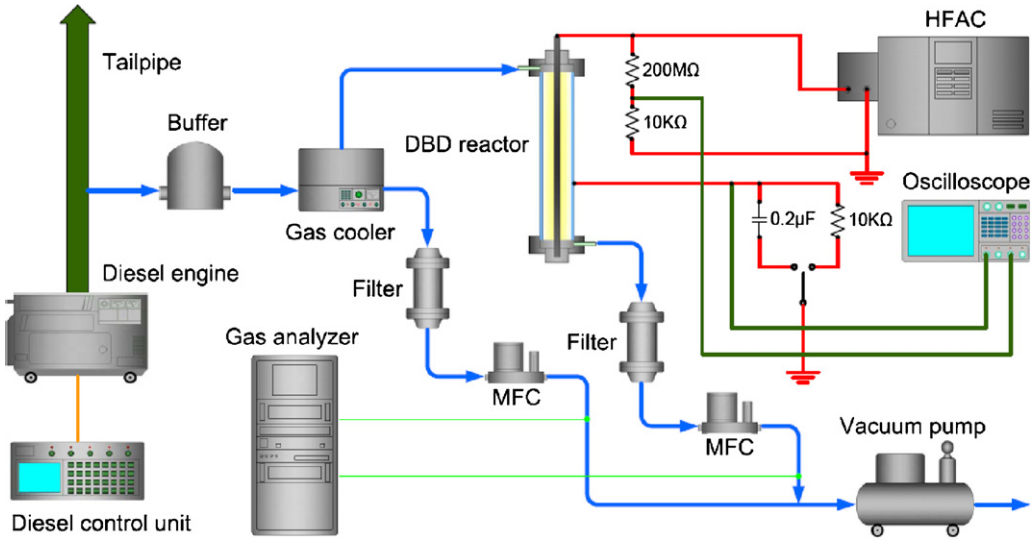

Fig. 1. Experimental setup.

ing cannot convert NO_2 into N_2, conversely, generates a significant amount of N_2O, HNO_3, and/or NO_3^- [15]. In this case, it is a better way to operate the plasma with lower voltage and a longer residence time [16]. According to Takaki et al. [17], NO_2 could be removed completely in the specific power range, but were produced again for too much power input. Furthermore, subsequent researches are being carried out for an attempt to NO_x removal in combination with catalysts [18–20].

The studies mentioned above clearly verify that a significant reduction in PM, HC and NO_x could be achieved by means of NTP processing. However, the simulated pure gas mixtures commonly have been used to estimate the removal efficiency. Although this strategy is beneficial to research the detailed mechanism and reaction pathways to pollutant reduction, the reduction efficiency is nonetheless different to be attained from that on real diesel running conditions, as the components in diesel exhaust emissions are complex and changeable with the variation of engine operation condition. On the other hand, free radicals, molecular dissociation and reactions induced by NTP processing acting on these components may give rise to the mutual and synergetic effects. Consequently, a precise knowledge of the actual reduction of diesel engine exhaust is essential for NTP technology.

The purpose of this work is to study the effect of NTP on the reduction in NO_x, HC and PM including carbon soot and soluble organic fraction (SOF) as a function of engine operating conditions. The results of this study provide an estimation to abate the diesel exhaust pollutants with NTP technology and are also helpful to accept NTP technology on diesel engine.

2. Experiment and measurement

2.1. Experimental setup

The experimental setup is shown in Fig. 1. The system mainly consists of an exhaust gas supply, DBD reactor, high frequency AC power supply (HFAC, the sine wave, peak voltage: 0–14 kV, frequency: 10–27 kHz), analytical systems and electrical measurement section. Exhaust gas was produced by an off-road diesel engine and sampled fractionally from the tailpipe by vacuum pump, which was set at the end of the line. The engine featured a 17.5:1 compression ratio, one cylinder, direct injection, air cooler, cylinder displacement of 296 mL and rated power of 2.4 kW at 3000 rpm. An indirect water-exchange cooler was used to regulate the temperature of exhaust gas prior to their entering into the DBD reactor. The desired flow rates were controlled by mass flow controllers (MFC) on each line, and the flow rate passing through the reactor was kept constant at 5 L/min for all experimental runs.

2.2. DBD reactor

A schematic of the DBD reactor in coaxial configuration is illustrated in Fig. 2. Two concentric quartz tubes were used for dielectric barrier layers with wall thickness of 1 mm. The outer and inner one had the outside diameters of 18 mm and 8 mm, respectively. Correspondingly, the discharge gap was fixed at 4 mm. The high-voltage (HV) electrode was placed on the axis center of quartz tubes using a stainless steel rod of 6 mm diameter, and connected to HFAC. We nickeled the ektexine of outer quartz tube as the ground electrode, 30 mm in width, making it possible to observe discharges in the gas gap.

2.3. Electrical circuit and measurement

The electrical measurements in discharges were performed using a digital oscilloscope (Tektronix, TDS1002, USA). The applied voltage was measured by a 1000:1 divider resistor connected in parallel with the discharge circuit, and the current was obtained from the voltage drop across a 10 kΩ sampling resistor connected in series with the ground line of DBD reactor. The determination of the power dissipated in DBD has often proved to be difficult because in reality the power is consumed in a large number of short-lived microdischarges [21]. In the experiment, the consumed energy during one discharge cycle was estimated from the voltage output and the accumulated charge through a *V*–*Q* Lissajous figure [22,23], using a 0.2 μF non-inductive capacitor inserted between

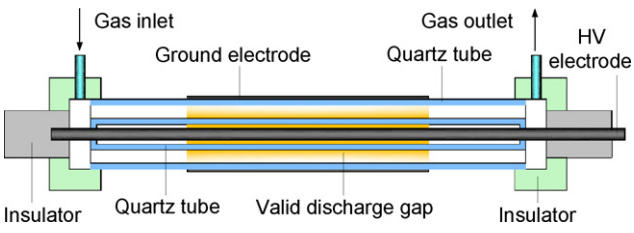

Fig. 2. The configuration of dielectric barrier discharge reactor.

Table 1
GC–MS analytical conditions.

Hewlett-Packard capillary column	HP-5, 12 m × 0.23 mm
Column oven temperature program	50 °C (5 min) → 25 °C (5 min) → 280 °C (4 min)
Injection/detector temperature	300 °C/300 °C
Carrier gas	Helium (flow rate 1.0 mL/min; head pressure 0.02 MPa)
Injection mode	Diffluent injection (diffluent proportion 30:1)
MS ion source	Electron-impact source
Ion source temperature	190 °C
Scan mass range	30–450 amu (full scan mode)

the reactor and the ground instead of the sampling resistor. Typically, the *V*–*Q* Lissajous figure is a parallelogram. The area of this parallelogram is equal to the energy dissipated during one period, and the average power consumed in discharges could be calculated by multiplying the discharge energy per one cycle by the operating frequency. The plasma process was evaluated by monitoring the removal efficiency of pollutant as a function of the specific energy density (SED), which was calculated by the following relation:

$$\text{specific energy density (J/L)} = \frac{\text{discharge power (W)}}{\text{gas flow rate (L/s)}}$$

2.4. Analytical methods

The raw and after-treated PM were directly sampled by the filters, and the PM mass on each filter was determined gravimetrically by the difference in mass before and after each test using an electronic analytical microbalance (Sartorius ME 5-F) with an accuracy of 0.001 mg. In order to separate the carbon soot and SOF, the collected samples of PM were extracted using the Soxhlet technique under yellow fluorescent lights. The samples were extracted with the methylene chloride as the solvent for 24 h. The resulting extracts were concentrated and then kept in the sealed bottles at −20 °C in the dark, respectively. The whole course of concentration was protected by nitrogen gas. When the methylene chloride volatilized completely, the dry filter papers were weighed. Then the mass of carbon soot as well as soluble organic fraction (SOF) was calculated according to the difference of the filter paper mass before and after the extraction. The morphology of PM was observed by scanning electron microscopy (XL30ESEM, Phlilps). Exhaust gases were measured by a gas analyzer (HORIBA MEXA 7500D, Japan): NO_x was analyzed by a chemiluminescent detector (CLD) and HC by a hot flame ionization detector (FID).

The componential analysis of SOF was undertaken with GC-MS (HP5890A-HP5971, USA) with a computer workstation. The GC–MS analytical conditions were shown in Table 1. The standard solutions of alkylic compounds and polycyclic aromatic hydrocarbons (PAHs) were used for identification and quantization. The alkylic compounds were determined by means of the scan mode and PAHs by means of selected ion monitoring mode.

3. Experimental results and discussion

3.1. Effect of peak voltage on contaminant abatements

HFAC power input plays a significant role in discharges, and the power consumption is varied by changing peak voltage and/or frequency [24]. The relations between peak voltage and discharge power are given in Fig. 3. Correspondingly, the abatement capabilities of PM, HC and NO_x as functions of voltage are illustrated in Fig. 4, where the applied frequency is fixed at 15.5 kHz and the engine runs at 50% load for these data. The PM, HC and NO_x concentrations in this diesel engine condition are 73.67 μg/L, 107.6 ppm and 476.3 ppm, respectively.

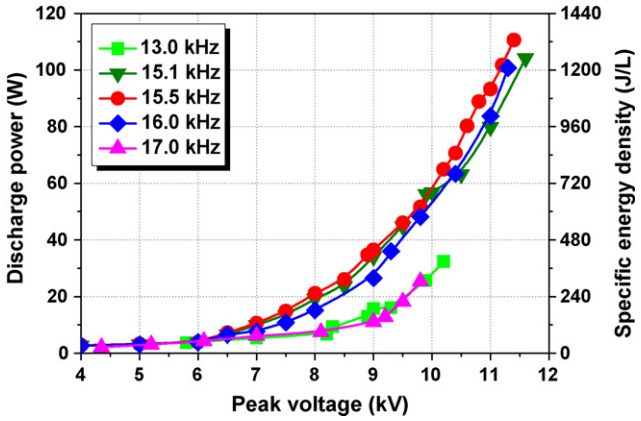

Fig. 3. Discharge power and specific energy density as a function of peak voltage.

As shown in Fig. 3, different discharge powers can be obtained under the different frequency conditions for a given voltage. Initially, the plasma does not exist since the peak voltage is lower than the breakdown voltage. As a result, the physical adsorption produced in the AC electric field is mainly responsible for the lower removal efficiency of contaminants (in Fig. 4). When the peak voltage exceeds the breakdown voltage, discharge power shows a monotonously increasing trend with the enhancement of peak voltage. At the applied frequencies of 15.1 kHz, 15.5 kHz and 16.0 kHz, the breakdown voltages demanded for plasma discharges are about 6 kV, while the frequencies of 13.0 kHz and 17.0 kHz correspond to the breakdown voltage of 9 kV. As the operating frequency is set at 15.5 kHz, obviously, the abatements of PM, HC and NO_x bring on obvious increases as the applied voltage is higher than the breakdown voltage of 6 kV (47 J/L).

For the PM removal, it can be seen that in the range of 6–8.5 kV the peak voltage is in direct proportion to the removal efficiency at the given frequency of 15.5 kHz. SEM analysis of PM appearance before and after treatments also gives information about the removal efficiency. Fig. 5(a) shows the SEM image of PM appearance before plasma treatment. A mass of agglomerates certified as the particulates of PM can be observed on the surface of most glass fibres. According to PM appearance after treatment at 8.5 kV (314 J/L) in Fig. 5(b), however, it can be seen that numbers of agglomerates decrease and the diameter of PM becomes smaller obviously than that before plasma treatment, which attests to the

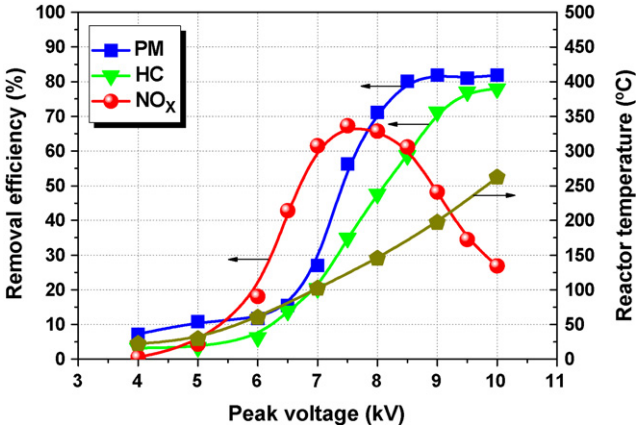

Fig. 4. PM, HC and NO_x removal efficiencies as a function of peak voltage (applied frequency = 15.5 kHz; engine load = 50%; initial PM concentration = 73.67 μg/L; initial HC concentration = 107.6 ppm; initial NO_x concentration = 476.3 ppm).

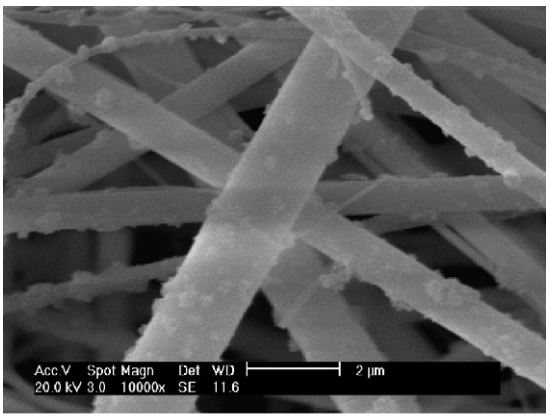

(a) Before treatment

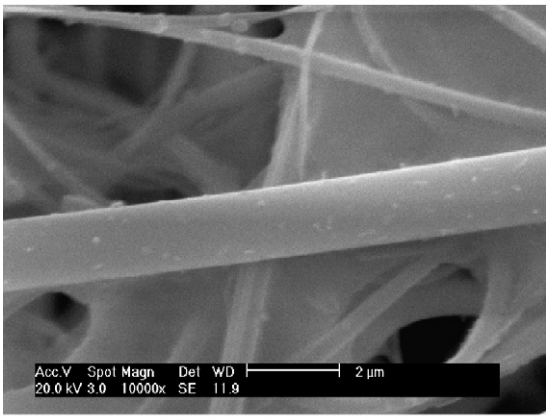

(b) After treatment

Fig. 5. SEM analysis of PM appearance before and after treatments. (a) Before treatment and (b) after treatment.

validity of PM removal by NTP process. At the value of 8.5 kV the removal efficiency levels off and approximately approaches to the maximum of 82%. Two reasons may be attributed to the saturation of removal efficiency. First, as shown in Fig. 4, there exists a systematic increase in the reactor temperature with increasing SED and more energy is converted into heat, resulting in the energy utilization efficiency for the DBD system decreasing; second, the high temperatures condition would induce segmental active particles such as ozone, which benefit the removal reaction, to decompose. As for the removal of HC, Fig. 4 illustrates the similar trend to that of PM. Namely, the removal efficiency for HC increases with the peak voltage from 4 kV to 10 kV (34–730 J/L) and the maximum of HC removal efficiency is around 78% at 10 kV. In addition, when the peak voltage exceeds 9 kV, the curve of removal efficiency for HC versus peak voltage also becomes smoother because of the two reasons mentioned above. Compared with the removal efficiency for HC, it is evident that superior removal efficiency for PM is achieved under the same experimental conditions. The difference in the removal efficiency is probably attributable to particle sizes between PM and HC. PM from diesel engine is mainly aggregates of spherical carbon soot coated by SOF, and its particle diameter is much larger than that of HC. The larger particle diameter, the easier to be attacked by electrons and radicals, and hence the higher removal efficiency for PM can be attained.

The NO_x removal efficiency as a function of voltage is also plotted in Fig. 4. It can be seen that the trend of NO_x is distinguished from that of PM and HC. In the range of 4–7.5 kV (34–178 J/L) in the peak voltage, a significant increase of NO_x removal efficiency from 0.5% to 67.3% is observed. However, on further enhancing the peak voltage from 7.5 kV to 10 kV, lower NO_x removal efficiency was attained. The possible reason is that the higher SED causes more N_2 in exhaust emissions decomposing into NO_x.

PM from diesel engine emissions mainly consists of carbon soot and absorbed soluble organic fraction (SOF). For the removal of carbon soot, there are two presumable routes by NTP: the first channel is a simple oxidation by means of O and OH radicals, which come from the electron-impact dissociation of oxygen and water vapor molecules [25]; the second one represents the interaction between NO_x and carbon soot [26,27]. Total hydrocarbons, including SOF and gaseous HC, initially react with O atoms produced in discharges, and afterwards a series of chain reactions occur. Finally, HC are mainly oxidized into CO and CO_2 [28]. NO_x reduction in plasma mainly belongs to oxidative process, in which O radicals oxidize NO to NO_2 [29]. Hydrocarbons are critical to enhance the selective partial oxidation of NO to NO_2 in plasma, in particular the existence of unsaturated hydrocarbons [28,30]. In the presence of water vapor molecules, reactions of NO_x with OH radicals further result in the formation of HNO_2 or HNO_3, which contribute to the leading NO_x reduction [15,27,30–32]. Strictly speaking, the conversion of NO_x into N_2 that occurs through the reaction with N radicals is rather limited. Combined with special SCR catalysts, the DBD can effectively eliminate the formation of HNO_2 or HNO_3 and simultaneously achieve a satisfying consequence for NO_x removal [33–35].

From the results presented above, it has been validated that simultaneous removals of PM, HC and NO_x intimately depend upon the SED. But, with the increase of SED, namely the increase of applied voltage, for a given frequency, the trends of contamination abatements of HC and PM appear to be different from that of NO_x. On the one hand, with the increase of SED the removals of PM and HC present the increasing trends and achieve a saturation value. On the other hand, the maximal removal efficiency for NO_x can be obtained at about 7.5 kV, however with the increase of SED going on the removal efficiency decreased due to the abruption of more nitrogen molecules. Hence, it is necessary that the operating conditions of DBD should be taken into account to achieve the optimal integrative abatements of PM, HC and NO_x from diesel engine emissions.

3.2. Effect of applied frequency on contaminant abatements

Typical frequencies operating for DBD are commonly employed in the ranges of 10–50 kHz. As shown in Fig. 6, increasing the frequency from 13 kHz to 15.1 kHz at four levels of given voltages enhances the discharge power, while the increases of frequency going on induce the decreases of discharge power. The effects

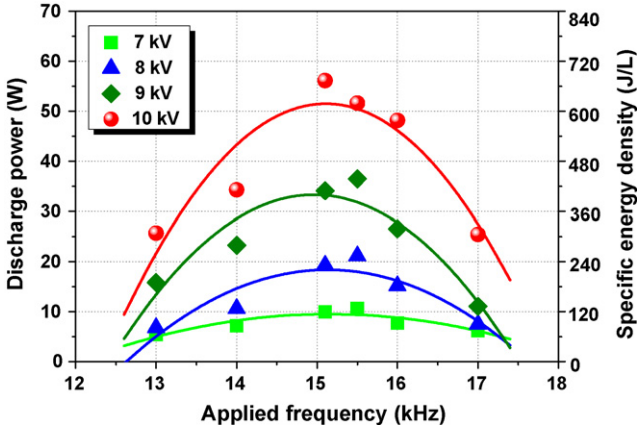

Fig. 6. Discharge power and specific energy density as a function of applied frequency.

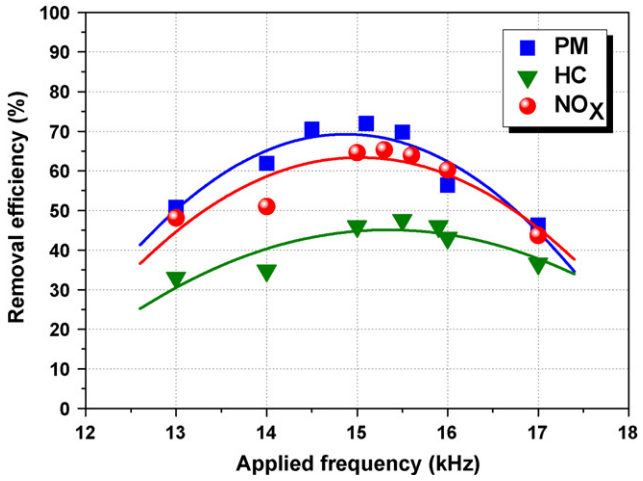

Fig. 7. Contaminant removal efficiencies as a function of applied frequency (peak voltage = 8 kV; engine load = 50%; initial PM concentration = 73.67 μg/L; initial HC concentration = 107.6 ppm; initial NO_x concentration = 476.3 ppm).

of applied frequency on contaminant abatements are presented in Fig. 7, where the peak voltage is controlled at 8 kV and the engine load is also set at 50%. It is obvious that the removal efficiencies for all contaminants as a function of applied frequency follow the similar trend of discharge power in Fig. 6. Videlicet, the removal efficiencies are augmented with the increases of applied frequency from 13 kHz to 15 kHz and then are reduced with the further increases of frequency. Approximately, at the same frequency of 15 kHz, the maximums of removal efficiencies are attained with 72% for PM, 47.6% for HC and 65% for NO_x, respectively. This phenomenon may be interpreted as follows: the total impedance for the circuit is determined by the operating frequency of HFAC. When the operating frequency approaches the resonance point, total impedance reaches the minimum. Simultaneously, the maximum of discharge power is obtained, leading to the highest removal efficiency. Above or below resonance point, on the other hand, the DBD system work at inductive and capacitive status respectively and the total impedance increases. As a result, the discharge power decreases and the removal efficiencies become low.

With respect to different DBD systems, the excellent discharge conditions usually appear to be different frequency bands, and therefore resonance points tend to be different, which are determined by the leakage inductances of power supplies and the resistance–capacitance loads of reactors. Several studies have also been conducted concerning the effects of DBD frequency on contaminant abatements. Mclarnon and Mathur [36] reported that NO_x conversion remarkably increased as the frequency was raised from 60 Hz to 1000 Hz at a given voltage. Also, Subrahmanyam et al. [37] obtained an increasing trend for the abatement of VOCs in the range of 200–300 Hz. Chavadej et al. [38], however, concluded that the benzene decomposition efficiency decreased substantially with the increase of frequency. The different conclusions presented by the literatures and our work may ascribe to the different frequency bands used in the experiments, viz. (i) below the resonance point, a increasing trend is observed, (ii) above the resonance point, a decreasing trend is observed.

3.3. Effect of engine load on contaminant abatements

Five different engine loads are used in this section, namely idle, 25%, 50%, 75% and 100% load respectively, and DBD system is run at resonance frequency (15.5 kHz). As a function of engine load, initial exhaust concentrations of NO_x, HC and PM including carbon soot and SOF are presented in Table 2. It is apparent that with the enhancement of engine loads, the concentrations of NO_x, PM and carbon soot increase, while those of HC and SOF decrease. The effects of peak voltage on the contaminant concentrations under various engine loads selected are illustrated in Figs. 8–11. All contaminant removals exhibit a strong correlation with the voltage applied. Compared with those without DBD, the concentrations of PM and HC are degressive from 0 kV to 10 kV in the ranges of 76.26–13.35 μg/L and 151.9–12.5 ppm with the maximum decreases of 81.9% and 84.5%, respectively. Correspondingly, those of carbon soot and SOF in PM also decrease from 43.83 μg/L to 0.05 μg/L and from 59.17 μg/L to 5.88 μg/L with the maximum reduction percentages of 98.8% and 82.1%, respectively. Likewise, this DBD system could substantially reduce the concentration of NO_x, however, for all engine loads the minimum value of NO_x concentration appears at the voltage of 8 kV, and are in the

Table 2
Exhaust concentrations of NO_x, HC and PM (carbon soot and SOF).

Engine load	NO_x (ppm)	HC (ppm)	PM		
			Carbon soot (μg/L)	SOF (μg/L)	Total (μg/L)
Idle	322.6	151.9	4.33	59.17	63.5
25%	433.2	126.1	10.92	56.67	67.59
50%	476.3	107.6	27.08	46.59	73.67
75%	504.6	93.2	36.42	38.71	75.13
100%	586.1	80.4	43.83	32.43	76.26

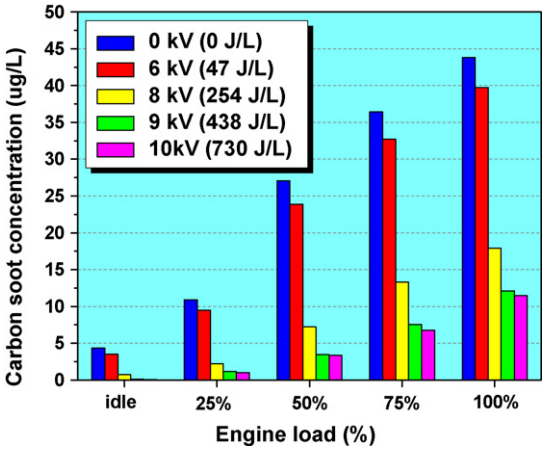

Fig. 8. Effects of peak voltage on carbon soot concentration under various loads.

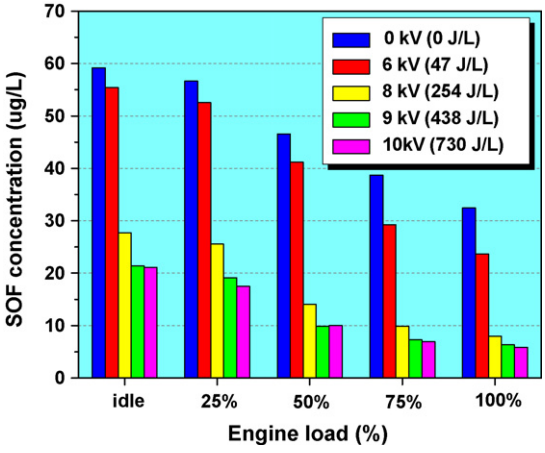

Fig. 9. Effects of peak voltage on SOF concentration under various loads.

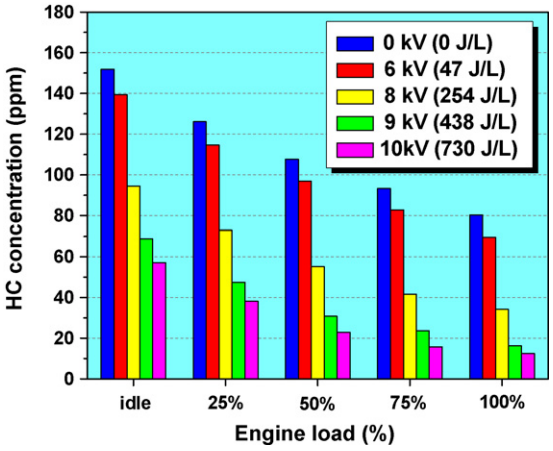

Fig. 10. Effects of peak voltage on HC concentration under various loads.

range of 586.1–90.0 ppm with the maximum removal efficiency of 71.8%. The explanations for the results above are in agreement with those relevant to HC, NO_x and PM removals mentioned in Section 3.1.

To compare the energy utilization efficiency of DBD system at different levels of peak voltage, the parameter of brake specific energy efficiency (BSEE) is introduced. The BSEE is calculated according to the following formula:

$$\text{BSEE} = \frac{C_A - C_B}{\text{SED}}$$

where C_A and C_B denotes the concentrations of contaminants with and without DBD (mg/L), respectively; SED represents the corresponding specific energy density (kJ/L).

The plots of BSEE for HC, NO_x and PM versus applied voltage at different engine loads are shown in Figs. 12–14. It is found that the BSEE for HC and NO_x is evidently reduced with the increase of applied voltage from 6 kV to 10 kV at all engine loads. That is, under the experimental conditions, the higher voltages for HC and NO_x abatement, the lower energy utilization efficiency of DBD system. With respect to the BSEE for PM, a similar trend is also observed at 75% and 100% engine loads, but for other engine loads (idle, 25% load and 50% load) the maximum of BSEE appears approximately at the applied voltage of 7.5 kV, where the highest energy utilization efficiency is obtained.

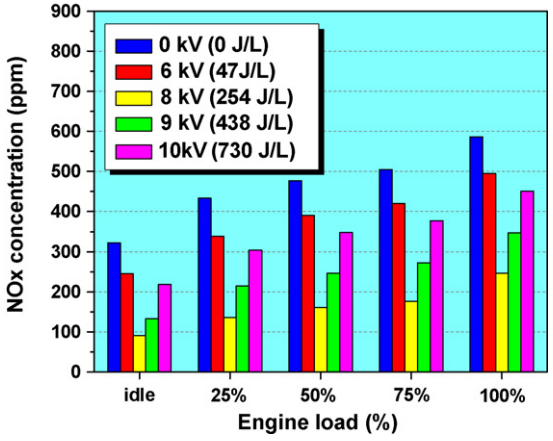

Fig. 11. Effects of peak voltage on NO_x concentration under various loads.

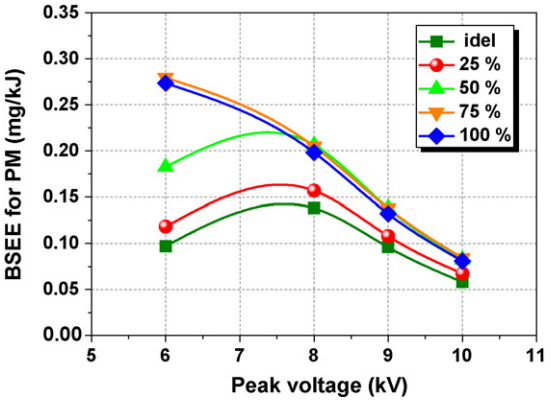

Fig. 12. BSEE for PM as a function of peak voltage.

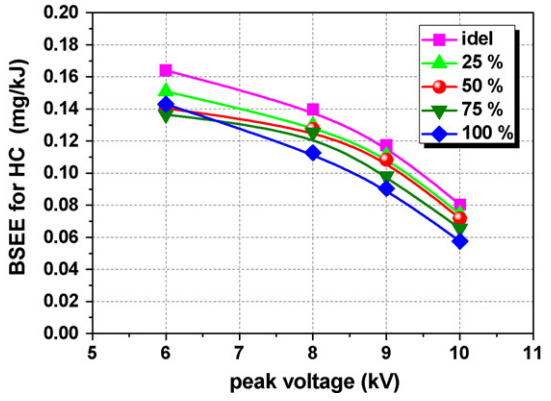

Fig. 13. BSEE for HC as a function of peak voltage.

3.4. Alkanes and polycyclic aromatic hydrocarbons abatements

Among the various compounds in exhaust emissions, 10 alkanes and 9 polycyclic aromatic hydrocarbons (PAHs) before and after treatment are quantified following extraction of samples collected on filters. These unregulated compounds are decane, dodecane, tridecane, tetradecane, cetane, heptadecane, octadecane, eicosane, docosane, tetracosane, phenanthrene, fluoranthene, pyrene, benzo[*a*]anthracene (B*a*A), chrysene, benzo[*b*]fluoranthene (B*b*F), benzo[*k*]fluoranthene (B*k*F), benzo[*a*]pyrene (B*a*P), benzo[*g*,*h*,*i*]perylene (B*ghi*P).

The removals of individual compounds selected are shown in Fig. 15, where the SED is controlled at 8.5 kV and 15.5 kHz (314 J/L), and the engine load is set at 50%. In most cases, the alkanes in

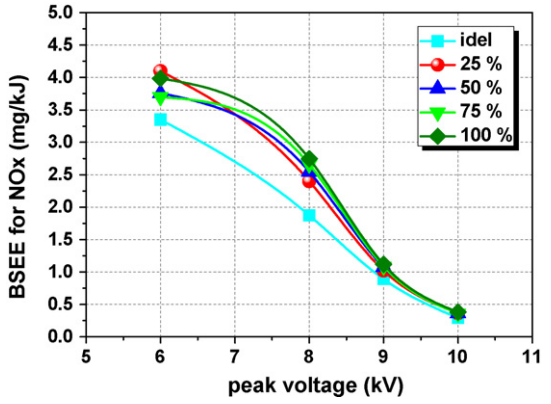

Fig. 14. BSEE for NO_x as a function of peak voltage.

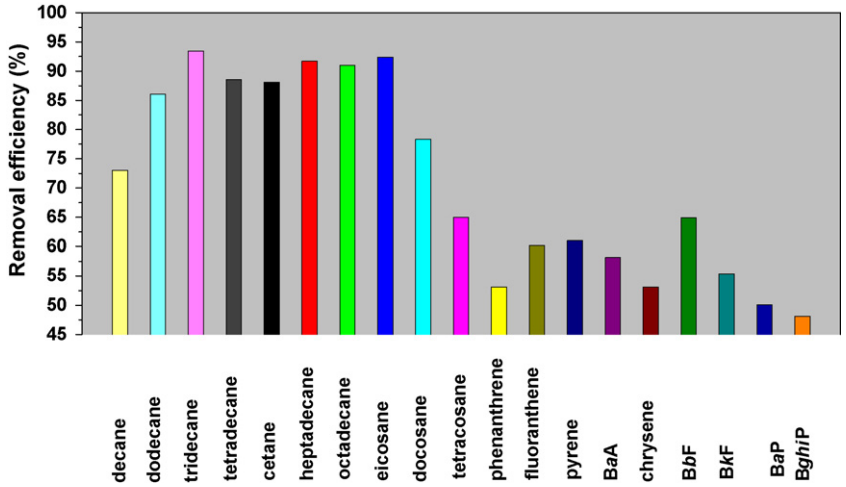

Fig. 15. Removal efficiencies of alkanes and PAHs.

exhaust emissions are easier to be removed than PAHs. The removal efficiencies of most alkanes could reach above 80% except for decane, docosane and tetracosane, while those of all PAHs were less than 65%. The bond energy in the molecules may be responsible for the different removal efficiencies. The bond energy in alkane molecule is weaker than that in PAH molecule, and more readily subjected to electronic attacks.

4. Conclusions

In this study, a series of DBD experiments have been implemented on the simultaneous removals of PM, HC and NO_x. The actual exhaust emissions from diesel engine are measured before and after treatment of the DBD system. Measurements exhibits a excellent performance of DBD: at the operating conditions, the maximums of PM, HC and NO_x removal efficiencies could reach more than 80%, 75% and 65%, respectively. For a specific frequency, the rise of peak voltage benefits the abatements of PM and HC, while a lower NO_x removal is attained at the higher voltage. The resonance of DBD system is the optimum frequency to generate plasma, at which the highest removal efficiencies can be achieved for a given voltage. At most engine loads, the energy utilization efficiency is reduced with the increase of peak voltage. As for the unregulated emissions, the alkanes in SOF are more easily removed than PAHs.

Although this paper provides a description of DBD effects on the simultaneous abatements of PM, HC and NO_x in the actual diesel exhaust environment, there are a number of aspects that should be investigated, such as the influence of the exhaust gas temperature, concentrations of water and oxygen in exhaust gases, the interactions of reactants, and combination with catalyst. In the future research, we will give more attentions to these aspects.

Acknowledgments

This study was supported by the National Key Basic Research and Development Program (2002CB211600) and the Program for New Century Excellent Talents in University (NCET-05-0244).

References

[1] P. Saiyasitpanich, T.C. Keener, S.-J. Khang, M. Lu, Removal of diesel particulate matter (DPM) in a tubular wet electrostatic precipitator, J. Electrostat. 65 (2007) 618–624.
[2] H. Miessner, K.-P. Francke, R. Rudolph, T. Hammer, NO_x removal in excess oxygen by plasma-enhanced selective catalytic reduction, Catal. Today 75 (2002) 325–330.
[3] N. Apostolescu, B. Geiger, K. Hizbullah, M.T. Jan, S. Kureti, D. Reichert, F. Schott, W. Weisweiler, Selective catalytic reduction of nitrogen oxides by ammonia on iron oxide catalysts, Appl. Catal. B: Environ. 62 (2006)104–114.
[4] K. Yoshida, M. Okubo, T. Yamamoto, Distinction between nonthermal plasma and thermal desorptions for NO_x and CO_2, Appl. Phys. Lett. 90 (2007) 131501.
[5] S. Sato, M. Kimura, T. Aki, I. Koyamoto, K. Takashima, S. Katsura, A. Mizuno, A removal system of diesel particulate using electrostatic precipitator with discharge plasma, in: Industry Applications Conference, 2005: Fourtieth IAS Annual Meeting, 2005, pp. 2203–2206.
[6] A. Yezerets, N.W. Currier, H.A. Eadler, A. Suresh, P.F. Madden, M.A. Branigin, Investigation of the oxidation behavior of diesel particulate matter, Catal. Today 88 (2003) 17–25.
[7] S. Masuda, S. Hosokawa, X.-L. Tu, K. Sakakibara, S. Kitoh, S. Sakai, Destruction of gaseous pollutants by surface-induced plasma chemical process (SPCS), IEEE Trans. Ind. Appl. 29 (1993) 781–786.
[8] S.V. Mitko, Y.B. Udalov, P.J.M. Peters, V.N. Ochkin, K.-J. Boller, Generation of powerful electron beams in a dense gas with a dielectric-barrier-discharge-based cathode, Appl. Phys. Lett. 83 (2003) 2760–2762.
[9] R. McAdams, Prospects for non-thermal atmospheric plasmas for pollution abatement, J. Phys. D: Appl. Phys. 34 (2001) 2810–2821.
[10] K. Takaki, T. Fujiwara, Multipoint barrier discharge process for removal of NO_x from diesel engine exhaust, IEEE Trans. Plasma Sci. 29 (2001) 518–523.
[11] S. Yao, C. Fushimi, K. Madokoro, K. Yamada, Uneven dielectric barrier discharge reactors for diesel particulate matter removal, Plasma Chem. Plasma Process. 26 (2006) 481–493.
[12] F. Willems, Y.C. Creyghton, C.V. Gulijk, H. Oonk, S. Maisuls, Experimental study into plasma-assisted PM removal for diesel engines, SAE paper 2003-01-1878.
[13] T. Koizumi, R. Ohyama, S. Okabe, An experimental NO_x treatment in diesel engine combustion exhaust gases by non-thermal plasma and activated carbon filter combinations, in: 2004 Annual Report Conference on Electrical Insulation and Dielectric Phenomena, 2004, pp. 130–134.
[14] D. Herling, M. Smith, S. Baskaran, Application of non-thermal plasma assisted catalyst technology for diesel engine emission reduction, SAE Paper 2003-01-3088.
[15] T. Yamamoto, C.-L. Yang, M.R. Beltran, Z. Kravets, Plasma-assisted chemical process for NO_x control, IEEE Trans. Ind. Appl. 36 (2000) 923–927.
[16] T. Yamamoto, Optimization of nonthermal plasma for the treatment of gas streams, J. Hazard. Mater. 67 (1999) 165–181.
[17] K. Takaki, M.A. Jani, T. Fujiwara, Removal of nitric oxide in flue gases by multipoint to plane dielectric barrier discharge, IEEE Trans. Plasma Sci. 27 (1999) 1137–1145.
[18] S. Bröer, T. Hammer, Selective catalytic reduction of nitrogen oxides by combining a non-thermal plasma and a V_2O_5-WO_3/TiO_2 catalyst, Appl. Catal. B: Environ. 28 (2000) 101–111.
[19] Y.H. Lee, J.W. Chung, Y.R. Choi, J.S. Chung, M.H. Cho, W. Namkung, NO_x removal characteristics in plasma plus catalyst hybrid process, Plasma Chem. Plasma Process. 24 (2004) 137–154.
[20] R.G. Tonkyn, S.E. Barlow, J.W. Hoard, Reduction of NO_x in synthetic diesel exhaust via two-step plasma-catalysis treatment, Appl. Catal. B: Environ. 40 (2003) 207–217.
[21] U. Kogelschatz, Dielectric-barrier discharges: their history, discharge physics, and industrial applications, Plasma Chem. Plasma Process. 23 (2003) 1–46.
[22] K. Takaki, J.-S. Chang, Atmospheric pressure of nitrogen plasmas in a ferroelectric packed bed barrier discharge reactor, IEEE Trans. Dielectr. Electr. Insul. 11 (2004) 481–490.
[23] R. Rudolph, K.-P. Francke, H. Miessner, OH radicals as oxidizing agent for the abatement of organic pollutants in gas flows by dielectric barrier discharges, Plasma Polym. 8 (2003) 153–161.

[24] B.-Y. Lee, S.-H. Park, S.-C. Lee, M. Kang, S.-J. Choung, Decomposition of benzene by using a discharge plasma–photocatalyst hybrid system, Catal. Today 93–95 (2004) 769–776.
[25] J.-O. Chae, Non-thermal plasma for diesel exhaust treatment, J. Electrostat. 57 (2003) 251–262.
[26] K. Hizbullah, S. Kureti, W. Weisweiler, Potassium promoted iron oxide catalysts for simultaneous catalytic removal of nitrogen oxides and soot from diesel exhaust gas, Catal. Today 93–95 (2004) 839–843.
[27] R. Dorai, M.J. Kushner, Repetitively pulsed plasma remediation of NO_x in soot laden exhaust using dielectric barrier discharges, J. Phys. D: Appl. Phys. 35 (2002) 2954–2968.
[28] A.R. Martin, J.T. Shawcross, J.C. Whitehead, Modelling of non-thermal plasma after treatment of exhaust gas streams, J. Phys. D: Appl. Phys. 37 (2004) 42–49.
[29] T. Yamamoto, B.S. Rajanikanth, M. Okubo, T. Kuroki, M. Nishino, Performance evaluation of nonthermal plasma reactors for NO oxidation in diesel engine exhaust gas treatment, IEEE Trans. Ind. Appl. 39 (2003) 1608–1613.
[30] B.M. Penetrante, R.M. Brusasco, B.T. Merritt, W.J. Pitz, G.E. Vogtlin, Feasibility of plasma after treatment for simultaneous control of NO_x and particulates, SAE Paper 1999-01-3637.
[31] R. Dorai, K. Hassouni, M.J. Kushner, Interaction between soot particles and NO_x during dielectric barrier discharge plasma remediation of simulated diesel exhaust, J. Appl. Phys. 88 (2000) 6060–6071.
[32] S. Yao, M. Okumoto, K. Madokoro, T. Yashima, Pulsed dielectric barrier discharge reactor for diesel particulate matter removal, J. AIChE 50 (2004) 1901–1907.
[33] J. Niu, X.F. Yang, A.M. Zhu, L.L. Shi, Q. Sun, Y. Xu, C. Shi, Plasma-assisted selective catalytic reduction of NO_x by C_2H_2 over Co-HZSM-5 catalyst, Catal. Commun. 7 (2006) 297–301.
[34] Y.S. Mok, H.-J. Lee, M. Dors, J. Mizeraczyk, Improvement in selective catalytic reduction of nitrogen oxides by using dielectric barrier discharge, J. Chem. Eng. 110 (2005) 79–85.
[35] Y. Itoh, M. Ueda, H. Shinjoh, M. Sugiura, M. Arakawa, NO_x reduction behavior on alumina with discharging nonthermal plasma in simulated oxidizing exhaust gas, J. Chem. Technol. Biot. 81 (2006) 544–552.
[36] C.R. McLarnon, V.K. Mathur, Nitrogen oxide decomposition by barrier discharge, Ind. Eng. Chem. Res. 39 (2000) 2779–2787.
[37] C. Subrahmanyam, A. Renken, L. Kiwi-Minsker, Novel catalytic non-thermal plasma reactor for the abatement of VOCs, J. Chem. Eng. 134 (2007) 78–83.
[38] S. Chavadej, W. Kiatubolpaiboon, P. Rangsunvigit, T. Sreethawong, A combined multistage corona discharge and catalytic system for gaseous benzene removal, J. Mol. Catal. A: Chem. 263 (2007) 128–136.